ELSEVIER

Journal of Organometallic Chemistry 565 (1998) 3–10

Journal of Organometallic Chemistry

Reversible coordination of the high oxidation state dioxo-acetylide fragment $(C_5Me_5)W(O)_2(CCPh)$ to a hexaruthenium cluster frame[1]

Wen-Ji Chao [a], Yun Chi [a,*], Cathy Chung [a], Arthur J. Carty [b], Esther Delgado [b], Shie-Ming Peng [c], Gene-Hsiang Lee [c]

[a] *Department of Chemistry, National Tsing Hua University, Hsinchu 30043, Taiwan, ROC*
[b] *Steacie Institute for Molecular Sciences, National Research Council Canada, 100 Sussex Drive, Ottawa, Ontario K1A 0R6, Canada*
[c] *Department of Chemistry and Instrumentation Center, National Taiwan University, Taipei 10764, Taiwan, ROC*

Received 22 October 1997

Abstract

Treatment of carbido cluster $Ru_6(\mu_6\text{-}C)(CO)_{17}$ with 3 equiv. of Me_3NO, followed by addition of high-valent acetylide complex $(C_5Me_5)W(O)_2(CCPh)$, affords a novel heterometallic cluster complex with formula $(C_5Me_5)W(O)_2(CCPh)Ru_6(\mu_6\text{-}C)(CO)_{14}$ (**1**). The $(C_5Me_5)W(O)_2(CCPh)$ fragment in this molecule, which serves as a six-electron-donor ligand, uses one of the W–O multiple bonds and the acetylide C–C triple bond to fill three adjacent coordination sites on the Ru_3 metal triangle of central $Ru_6(\mu_6\text{-}C)$ framework. Thermolysis of **1** in toluene leads to the formation of a toluene substituted complex $(C_5Me_5)W(O)_2(CCPh)Ru_6(\mu_6\text{-}C)(CO)_{11}(C_7H_8)$ (**2**) which exhibits the same metal core arrangement as its precursor **1**. In addition, the X-ray structural analysis reveals the evidence for extensive hydrogen bonding between the terminal oxo ligand and the methanol solvate present in the unit cell. © 1998 Elsevier Science S.A. All rights reserved.

Keywords: Heterometallic cluster; Tungsten; Ruthenium; Acetylide

1. Introduction

Not only low-valent carbonyl complexes but also high-valent oxide species are important reagents in various catalytic or stoichiometric chemical processes, although they are usually considered to be at opposite extremes of the spectrum of transition-metal organometallic compounds [1]. In view of their distinctive properties we were attracted to examine the metal cluster compounds containing both the low-oxidation-state metal carbonyl fragment and the high-oxidation-state metal oxide fragment. Although the number of these cluster complexes is rather limited, some studies on the carbonyl clusters with metal atom bearing bridging oxo ligand have been documented [2]. The simplest and most well-known examples involves $[Os(CO)_3(\mu_3\text{-}O)]_4$ [3], $Os_6(CO)_{17}(\mu_3\text{-}O)$ [4], $[Fe_3Mn(CO)_{12}(\mu_4\text{-}O)][PPN]$ and $[Fe_2Ru_3(CO)_{14}(\mu_4\text{-}O)][PPN]_2$ [5], in which the oxo ligand is bound to the metal atoms in a manner not different from other main group elements like carbide or nitride ligands. In addition, Shapley and coworkers have reported on the synthesis of heterometallic oxo complex with formula $CpW(\mu\text{-}O)Os_3(\mu_3\text{-}CCH_2Tol)(CO)_9$ [6], produced by the direct C–O bond cleavage of an acyl functional group, while Stone and coworkers [7] and Chi and coworkers [8] have obtained independently the respective tungsten–rhenium mixed-metal oxo complexes through direct air oxidation. Examination of the chemistry in these heterometallic oxo complexes reveals that the oxo ligand is able to promote the addition reaction by alternating its bonding between the terminal and the edge-bridging modes [6,9].

* Corresponding author. Fax: +886 3 5720864; e-mail: ychi@faculty.nthu.edu.tw

[1] Dedicated to Professor Michael I. Bruce on the occasion of his 60th bithday.

0022-328X/98/$19.00 © 1998 Elsevier Science S.A. All rights reserved.
PII S0022-328X(98)00439-2

In this study, we wish to report the synthesis of a cluster compound $(C_5Me_5)W(O)_2(CCPh)Ru_6(\mu_6\text{-}C)(CO)_{14}$ (**1**), directly from a mononuclear tungsten dioxo complex $(C_5Me_5)W(O)_2(CCPh)$ and a ruthenium carbido cluster complex $Ru_6(\mu_6\text{-}C)(CO)_{17}$. As complex **2** inherits the $(C_5Me_5)W(O)_2$ fragment; therefore, its bonding and reactivity pattern observed would also highlight the corresponding structural as well as chemical properties of oxo ligand on the high oxidation-state tungsten atom.

2. Experimental section

2.1. General information and materials

Infrared spectra were recorded on a Perkin-Elmer 2000 FT-IR spectrometer. ^{1}H- and ^{13}C-NMR spectra were recorded on either a Bruker AM-400 or a Varian Unity-400 instrument. ^{1}H- and ^{13}C-NMR chemical shifts are quoted with respect to internal standard tetramethylsilane. Mass spectra were obtained on a JEOL-HX110 instrument operating in fast atom bombardment (FAB) mode. The acetylide complex $(C_5Me_5)W(O)_2(CCPh)$ and carbido complex $Ru_6(\mu_6\text{-}C)(CO)_{17}$ were prepared according to literature procedures [10]. All reactions were performed under a nitrogen atmosphere using dried and deoxygenated solvents. The reactions were monitored by analytical thin-layer chromatography (5735 Kieselgel 60 F_{254}, E. Merck) and the products were separated on preparative thin-layer chromatographic plates (Kieselgel 60 F_{254}, E. Merck). Elemental analyses were carried out at the Regional Instrumentation Center at National Cheng Kung University, Tainan, Taiwan.

2.2. Reaction of $Ru_6(\mu_6\text{-}C)(CO)_{17}$ with $(C_5Me_5)W(O)_2(CCPh)$

An acetonitrile solution (20 ml) of freshly sublimed Me_3NO (34.2 mg, 0.447 mmol) was added dropwise into a CH_2Cl_2 solution (30 ml) of $Ru_6(\mu_6\text{-}C)(CO)_{17}$ (200 mg, 0.182 mmol) over a period of 30 min. Then the solvent was removed under vacuum, the acetylide complex $(C_5Me_5)W(O)_2(CCPh)$ (70 mg, 0.155 mmol) was added and the mixture was taken up in 60 ml of CH_2Cl_2. The solution was stirred at r.t. for 5 h during which the color changed to dark-brown. The solvent was removed and the residue was redissolved in minimum amount of CH_2Cl_2 and separated by thin-layer chromatography. Development with pure dichloromethane produced a brown band, which was extracted from silica gel to yield 135 mg of $(C_5Me_5)W(O)_2(CCPh)Ru_6(\mu_6\text{-}C)(CO)_{14}$ (**1**, 0.092 mmol, 51%). Crystals suitable for X-ray diffraction studies were obtained from a mixture of CH_2Cl_2 and methanol at r.t.

Selected spectral data for **1**: FAB MS (^{184}W, ^{102}Ru): m/z 1467 (M^+). IR (C_6H_{12}): ν(CO), 2079 (m), 2045 (s), 2039 (s), 2027 (m), 2018 (m), 1996 (br, w) cm^{-1}. ^{1}H-NMR (300 MHz, $CDCl_3$, 295 K): δ 2.02 (s, 15H, C_5Me_5), 7.46 (t, 1H, J_{HH} = 7.8 Hz), 7.58 (t, 2H, J_{HH} = 7.8 Hz), 7.96 (d, 2H, J_{HH} = 7.8 Hz). ^{13}C-NMR (75 MHz, CD_2Cl_2, 295 K): δ 11.9 ($C_5\mathit{Me}_5$), 119.5 (C_5Me_5), 129.7 (m,o-C_6H_5), 130.2 (p-C_6H_5), 130.8 (o,m-C_6H_5), 147.5 (i-C_6H_5), 159.6 (CCPh), 201.6 (CCPh), 431.4 (μ_6-C). Anal. Calcd for $C_{33}H_{20}O_{16}WRu_6$: C, 27.10; H, 1.38. Found: C, 27.21; H, 1.42.

2.3. Treatment of *1* with CO

A toluene solution (30 ml) of **1** (22 mg, 0.015 mmol) was heated at 110°C under CO atmosphere for 25 min, during which the color changed from brown to light brown. After the removal of solvent, the residue was redissolved in CH_2Cl_2 and separated by thin-layer chromatography. Development with pure dichloromethane produced two major bands, which were extracted from silica gel to yield 14.1 mg of orange $Ru_6(\mu_6\text{-}C)(CO)_{17}$

Table 1
X-ray structural data of complexes **1** and **2**

Compound	**1**	**2**
Formula	$C_{33}H_{20}O_{16}Ru_6W$	$C_{37}H_{28}O_{13}Ru_6W\cdot CH_3OH$
Molecular weight	1462.77	1502.92
Crystal system	Orthorhombic	Orthorhombic
Space group	P_{bca}	P_{bca}
Unit cell dimensions		
a (Å)	16.883(2)	14.307(3)
b (Å)	17.856(3)	20.340(2)
c (Å)	26.478(2)	29.058(3)
Volume (Å^3)	7982(2)	8456(2)
Z	8	8
D_{calc} (g cm^{-3})	2.434	2.361
F(000)	5397	5605
2θ (max) (°)	50.0	50.0
$h\ k\ l$ ranges	0 20, 0 21, 0 31	0 16, 0 24, 0 34
Crystal size (mm)	$0.30\times0.40\times0.50$	$0.13\times0.20\times0.40$
μ(Mo–K$_\alpha$) cm^{-1}	48.04	76.40
Transmission: max, min.	1.000, 0.644	1.000, 0.912
No. of data in refinement, $I\geq2\sigma(I)$	4830	4349
No. of atoms and parameters	76, 506	91, 533
Weight modifier (g)	0.00005	0.0001
Maximum Δ/σ ratio	0.003	0.008
R_F; R_w	0.030; 0.030	0.041; 0.034
GOF	1.46	1.20
D-map, max./min (eÅ^{-3})	0.75/−0.81	0.95/−1.23

Features common to all determinations: Nonius CAD-4 diffractometer, λ(Mo–K$_\alpha$) = 0.7107 Å; minimize function: $\Sigma(w|F_o-F_c|^2)$, weighting scheme: $w^{-1}=\sigma^2(F_o)+|g|\ F_o^2$; GOF = $[\Sigma w|F_o-F_c|^2/(N_o-N_v)]^{1/2}$ (N_o = number of observations; N_v = number of variables).

Table 2
Selected bond distances (Å) and angles (°) of **1** (esd. in parentheses)

Metal–metal distances			
W–Ru(1)	2.8024(8)	Ru(1)–Ru(2)	2.8191(9)
Ru(1)–Ru(3)	2.846(1)	Ru(1)–Ru(5)	2.907(1)
Ru(1)–Ru(6)	2.8837(9)	Ru(2)–Ru(3)	2.7364(9)
Ru(2)–Ru(4)	2.875(1)	Ru(2)–Ru(6)	3.030(1)
Ru(3)–Ru(4)	2.924(1)	Ru(3)–Ru(5)	2.933(1)
Ru(4)–Ru(5)	2.893(1)	Ru(4)–Ru(6)	2.879(1)
Ru(5)–Ru(6)	2.851(1)		
Metal–carbide atom distances			
Ru(1)–C(15)	1.997(7)	Ru(2)–C(15)	2.025(7)
Ru(3)–C(15)	2.038(7)	Ru(4)–C(15)	2.057(7)
Ru(5)–C(15)	2.047(7)	Ru(6)–C(15)	2.062(7)
Metal–acetylide ligand distances and angles			
W–C(16)	2.031(8)	Ru(1)–C(16)	2.130(8)
Ru(2)–C(16)	2.269(7)	Ru(2)–C(17)	2.206(7)
Ru(3)–C(17)	2.073(7)	C(16)–C(17)	1.38(1)
∠W–C(16)–C(17)	156.2(6)	∠C(16)–C(17)–C(18)	126.4(7)
Meta3–oxo ligand distances and angles			
W–O(15)	1.810(6)	W–O(16)	1.711(6)
Ru(1)–O(15)	2.156(6)		
∠O(15)–W–O(16)	107.2(3)	∠Ru(1)–O(15)–W	89.5(2)

(0.013 mmol, 86%) and 6 mg of light yellow $(C_5Me_5)W(O)_2(CCPh)$ (0.013 mmol, 90%).

2.4. Thermolysis of $(C_5Me_5)W(O)_2(CCPh)Ru_6(\mu_6\text{-}C)(CO)_{14}$

A toluene solution (60 ml) of **1** (120 mg, 0.082 mmol) was stirred at reflux for 8 h, during which time no obvious change of color was observed. After the removal of solvent in vacuo, the residue was taken up in CH_2Cl_2 and separated by thin-layer chromatography using pure dichloromethane as eluent, affording 58 mg of $(C_5Me_5)W(O)_2(CCPh)Ru_6(\mu_6\text{-}C)(CO)_{11}(C_7H_8)$ (**2**, 0.039 mmol, 48%). Single crystals of **2**, which contain one methanol solvent molecule, were obtained from a mixture of CH_2Cl_2 and methanol at room temperature.

Selected spectral data for **2**: FAB MS (^{184}W, ^{102}Ru): m/z 1475 (M^+). IR (C_6H_{12}): ν(CO), 2046 (s), 2013 (vs), 2001 (s), 1978 (s), 1946 (m), 1863 (br, w), 1789 (br, w) cm^{-1}. ^{1}H-NMR (400 MHz, $CDCl_3$, 295 K): δ 1.97 (s, 15H, C_5Me_5), 2.38 (s, 3H, Me), 5.39 (t, 1H, $J_{HH} = 6.0$ Hz), 5.60 (d, 1H, $J_{HH} = 6.0$ Hz), 5.62 (d, 1H, $J_{HH} = 6.0$ Hz), 5.69 (t, 1H, $J_{HH} = 6.0$ Hz), 5.73 (t, 1H, $J_{HH} = 6.0$ Hz), 7.38 (t, 1H, $J_{HH} = 7.5$ Hz), 7.50 (t, 2H, $J_{HH} = 7.5$ Hz), 7.96 (d, 2H, $J_{HH} = 7.5$ Hz). ^{13}C NMR (75 MHz, CD_2Cl_2, 295 K): δ 11.2 ($C_5\mathit{Me}_5$), 22.2 (Me), 83.5 (MeC_6H_5), 84.7 (MeC_6H_5), 85.8 (MeC_6H_5), 88.7 (MeC_6H_5), 90.7 (MeC_6H_5), 103.4 (MeC_6H_5), 118.1 (C_5Me_5), 128.5 (m,o-C_6H_5), 129.0 (p-C_6H_5), 130.6 (o,m-C_6H_5), 146.7 (i-C_6H_5), 156.4 (C*C*Ph), 193.9 (1CO), 195.7 (2CO), 198.6 (1CO), 199.7 (2CO), 199.8 (*C*CPh), 203.0 (3CO, br), 209.5 (3CO), 409.0 (μ_6-C). Anal. Calcd for $C_{37}H_{28}O_{13}WRu_6$: C, 30.21; H, 1.92. Found: C, 30.24; H, 1.98.

2.5. X-ray crystallography

The X-ray diffraction measurements were carried out on a Nonius CAD-4 diffractometer. Lattice parameters were determined from 25 randomly selected high-angle reflections. Three standard reflections were monitored every 3600 s. For complex **1**, no significant change in intensities was observed over the course of data collection. On the other hand, the intensity of the standard reflections of **2** reduced 12% during the data collection, which is presumably caused by the slow decomposition of crystal through loss of methanol solvate. The diffraction signals were then corrected for Lorentz, polarization and absorption effects (ψ scans). The structure was determined by using the NRCC-SDP-VAX package. The non-hydrogen atoms were allowed anisotropic temperature factors, and the hydrogen atoms were placed at the idealized positions with $U_H = U_C + 0.1$. The crystallographic refinement parameters of complexes **1** and **2** are given in Table 1, while their selected bond distances and angles and the atomic coordinates are presented in Tables 2–5, respectively. Other unessential bond distances and angles, tables of anisotropic thermal parameters and listings of the observed and calcu-

Table 3
Selected bond distances (Å) and angles (deg) of 2 (esd. in parentheses)

Metal–metal distances			
W–Ru(5)	2.831(1)	Ru(1)–Ru(2)	2.869(1)
Ru(1)–Ru(4)	2.866(1)	Ru(1)–Ru(5)	2.891(1)
Ru(1)–Ru(6)	2.928(1)	Ru(2)–Ru(3)	2.729(1)
Ru(2)–Ru(5)	3.002(1)	Ru(2)–Ru(6)	2.930(1)
Ru(3)–Ru(4)	3.006(1)	Ru(3)–Ru(5)	2.779(1)
Ru(3)–Ru(6)	2.899(1)	Ru(4)–Ru(5)	2.854(1)
Ru(4)–Ru(6)	2.815(1)		
Metal–carbide atom distances			
Ru(1)–C(12)	1.94(1)	Ru(2)–C(12)	2.02(1)
Ru(3)–C(12)	2.07(1)	Ru(4)–C(12)	2.08(1)
Ru(5)–C(12)	2.03(1)	Ru(6)–C(12)	2.09(1)
Metal–acetylide ligand distances and angles			
W–C(13)	2.03(1)	Ru(3)–C(13)	2.23(1)
Ru(5)–C(13)	2.20(1)	Ru(2)–C(14)	2.05(1)
Ru(3)–C(14)	2.23(1)	C(13)–C(14)	1.38(2)
∠W–C(13)–C(14)	148.3(8)	∠C(13)–C(14)–C(15)	128(1)
Metal–oxo ligand distances and angles			
W–O(12)	1.802(7)	W–O(13)	1.719(7)
Ru(5)–O(12)	2.170(7)	O(13)–O(14)	2.92(1)
∠O(12)–W–O(13)	106.9(3)	∠Ru(5)–O(12)–W	90.5(3)
Metal–toluene ligand distances			
Ru(1)–C(21)	2.23(1)	Ru(1)–C(22)	2.23(1)
Ru(1)–C(23)	2.21(1)	Ru(1)–C(24)	2.23(1)
Ru(1)–C(25)	2.25(1)	Ru(1)–C(26)	2.26(1)

Table 4
Atomic coordinates and isotropic displacement coefficients for complex **1**; e.s.ds. refer to the last digit printed

	x	*y*	*z*	B_{eq}
W	0.629866(23)	0.182854(21)	0.027363(13)	2.807(15)
Ru1	0.56046(4)	0.15579(4)	0.121755(25)	2.10(3)
Ru2	0.68188(4)	0.25108(4)	0.156556(25)	1.97(3)
Ru3	0.52798(4)	0.29460(4)	0.17032(3)	2.09(3)
Ru4	0.61983(4)	0.24430(4)	0.25756(3)	2.34(3)
Ru5	0.48933(4)	0.15378(4)	0.22172(3)	2.27(3)
Ru6	0.64804(4)	0.10310(4)	0.20824(3)	2.29(3)
C1	0.4545(5)	0.1432(5)	0.1045(3)	3.4(4)
C2	0.7796(5)	0.2170(5)	0.1295(3)	3.3(4)
C3	0.7382(5)	0.3366(5)	0.1775(3)	3.1(4)
C4	0.4308(5)	0.3300(5)	0.1415(3)	3.0(4)
C5	0.5416(5)	0.3833(5)	0.2059(3)	3.0(4)
C6	0.6861(5)	0.3228(5)	0.2795(3)	3.4(4)
C7	0.5529(5)	0.2657(5)	0.3125(3)	3.7(5)
C8	0.6842(5)	0.1657(5)	0.2876(4)	4.2(5)
C9	0.4079(5)	0.2276(5)	0.2308(4)	3.7(5)
C10	0.4906(5)	0.1173(5)	0.2874(3)	3.5(4)
C11	0.4202(5)	0.0748(5)	0.2022(3)	3.4(4)
C12	0.6348(5)	0.0210(5)	0.2530(3)	3.3(4)
C13	0.7542(5)	0.0769(5)	0.1958(3)	3.3(4)
C14	0.6019(6)	0.0392(5)	0.1523(4)	3.7(5)
C15	0.5879(4)	0.1994(4)	0.1890(3)	1.7(3)
C16	0.6062(4)	0.2532(4)	0.0857(3)	2.1(3)
C17	0.6021(4)	0.3211(4)	0.1105(3)	2.1(3)
C18	0.6247(5)	0.3947(4)	0.0898(3)	2.6(4)
C19	0.7002(5)	0.4061(5)	0.0688(4)	3.6(4)
C20	0.7218(6)	0.4733(6)	0.0480(4)	4.6(5)
C21	0.6683(7)	0.5312(5)	0.0470(4)	5.2(6)
C22	0.5943(7)	0.5216(5)	0.0684(4)	5.7(6)
C23	0.5737(5)	0.4549(5)	0.0888(4)	4.1(5)
C24	0.6345(6)	0.2159(6)	−0.0584(3)	4.4(5)
C25	0.5902(5)	0.2741(5)	−0.0365(3)	3.7(4)
C26	0.5178(5)	0.2412(5)	−0.0188(3)	3.6(4)
C27	0.5181(6)	0.1650(5)	−0.0307(3)	4.3(5)
C28	0.5915(6)	0.1486(5)	−0.0539(3)	4.4(5)
C29	0.7139(7)	0.2263(8)	−0.0830(4)	7.1(7)
C30	0.6079(7)	0.3560(6)	−0.0391(4)	5.7(6)
C31	0.4493(6)	0.2838(6)	0.0045(4)	5.6(6)
C32	0.4543(8)	0.1101(7)	−0.0232(4)	7.6(7)
C33	0.6172(10)	0.0737(7)	−0.0748(5)	9.4(10)
O1	0.3885(4)	0.1406(4)	0.0945(3)	5.7(4)
O2	0.8403(4)	0.1992(4)	0.1146(3)	5.1(4)
O3	0.7722(4)	0.3910(4)	0.1865(3)	5.2(4)
O4	0.3747(4)	0.3529(4)	0.1233(3)	6.2(4)
O5	0.5499(4)	0.4394(4)	0.2263(3)	5.4(4)
O6	0.7232(4)	0.3702(4)	0.2957(3)	5.4(4)
O7	0.5131(4)	0.2810(5)	0.3456(3)	6.9(4)
O8	0.7229(5)	0.1417(4)	0.3184(3)	6.3(4)
O9	0.3557(4)	0.2625(4)	0.2435(3)	6.7(4)
O10	0.4931(4)	0.0953(4)	0.328382(3)	5.0(4)
O11	0.3786(4)	0.0279(4)	0.1895(3)	5.7(4)
O12	0.6276(4)	−0.0272(4)	0.2800(3)	5.8(4)
O13	0.8180(4)	0.0593(4)	0.1900(3)	5.5(4)
O14	0.5912(5)	−0.0182(3)	0.1356(3)	5.7(4)
O15	0.6003(4)	0.0952(3)	0.056082(2)	4.0(3)
O16	0.7310(4)	0.1824(4)	0.023612(3)	4.6(3)

Table 5
Atomic coordinates and isotropic displacement coefficients for complex **2**; e.s.ds. refer to the last digit printed

	x	*y*	*z*	B_{eq}
W	0.42711(3)	0.2196732(3)	0.0317321(7)	2.0631(9)
Ru1	0.45022(6)	0.43021(4)	0.15646(4)	2.31(4)
Ru2	0.54346(6)	0.30567(4)	0.16294(3)	2.01(4)
Ru3	0.37770(6)	0.23986(4)	0.15663(3)	2.05(4)
Ru4	0.27102(6)	0.36718(5)	0.15634(4)	2.37(4)
Ru5	0.40487(6)	0.33256(4)	0.08768(3)	1.98(4)
Ru6	0.39496(7)	0.33766(5)	0.22869(3)	2.49(4)
C1	0.2701(8)	0.3742(5)	0.0837(4)	2.8(5)
C2	0.6618(8)	0.3393(6)	0.1462(4)	3.1(6)
C3	0.5919(7)	0.2722(5)	0.2179(4)	2.7(6)
C4	0.2705(9)	0.1966(6)	0.1307(4)	3.9(7)
C5	0.3836(9)	0.1751(6)	0.2035(4)	3.6(6)
C6	0.1559(8)	0.3183(6)	0.1543(4)	3.3(6)
C7	0.2095(8)	0.4496(6)	0.1552(4)	3.5(6)
C8	0.2681(8)	0.3790(6)	0.2315(4)	2.7(6)
C9	0.4598(9)	0.3972(5)	0.0498(4)	3.1(6)
C10	0.4542(9)	0.3877(6)	0.2741(4)	3.7(6)
C11	0.3690(9)	0.2766(6)	0.2755(4)	3.8(7)
C12	0.4109(7)	0.3389(5)	0.1573(4)	2.1(5)
C13	0.4741(7)	0.2371(5)	0.0966(4)	1.7(5)
C14	0.5225(7)	0.2147(5)	0.1346(4)	2.1(5)
C15	0.5685(8)	0.1500(5)	0.1407(4)	2.6(5)
C16	0.5231(8)	0.0925(6)	0.1257(4)	3.1(6)
C17	0.5705(10)	0.0329(5)	0.1276(5)	4.2(7)
C18	0.6617(9)	0.0296(6)	0.1424(5)	4.6(7)
C19	0.7055(8)	0.0859(7)	0.1566(5)	4.5(7)
C20	0.6597(8)	0.1457(6)	0.1569(5)	3.4(6)
C21	0.5170(10)	0.5027(6)	0.2035(4)	4.4(7)
C22	0.5824(9)	0.4852(5)	0.1696(5)	3.6(6)
C23	0.5559(9)	0.4939(5)	0.1232(5)	3.8(6)
C24	0.4664(10)	0.5197(6)	0.1126(5)	4.3(7)
C25	0.4064(9)	0.5357(6)	0.1473(5)	4.6(8)
C26	0.4292(10)	0.5268(6)	0.1938(5)	4.1(7)
C27	0.36571(2)	0.5472(7)	0.2310(6)	7.2(10)
C28	0.4721(8)	0.1940(6)	−0.0417(4)	2.9(6)
C29	0.5269(8)	0.1520(5)	−0.0133(4)	2.4(5)
C30	0.5898(7)	0.1914(5)	0.0113(4)	2.2(5)
C31	0.5783(7)	0.2570(5)	−0.0035(4)	2.6(5)
C32	0.5083(8)	0.2588(6)	−0.0369(4)	3.2(6)
C33	0.4004(9)	0.1727(7)	−0.0760(5)	5.2(8)
C34	0.5186(10)	0.0792(6)	−0.0099(5)	4.3(7)
C35	0.6665(8)	0.1708(7)	0.0427(4)	4.2(7)
C36	0.6407(9)	0.3136(7)	0.0101(5)	4.6(7)
C37	0.4726(10)	0.3170(6)	−0.0647(5)	5.0(8)
O1	0.2182(6)	0.3883(4)	0.0554(3)	4.5(5)
O2	0.7312(6)	0.3608(5)	0.1349(3)	5.7(5)
O3	0.6225(7)	0.2481(4)	0.2497(3)	5.2(5)
O4	0.2083(6)	0.1702(5)	0.1158(4)	5.9(6)
O5	0.3905(8)	0.1322(4)	0.2292(3)	6.1(6)
O6	0.0862(6)	0.2909(5)	0.1521(3)	5.5(5)
O7	0.1719(6)	0.4992(4)	0.1547(4)	6.1(6)
O8	0.2142(6)	0.4015(4)	0.2562(3)	4.3(5)
O9	0.4899(7)	0.4344(4)	0.0241(3)	5.1(5)
O10	0.4886(7)	0.4170(5)	0.3025(3)	6.0(5)
O11	0.3523(8)	0.2392(5)	0.3040(3)	6.7(6)
O12	0.3513(5)	0.2896(4)	0.0246(3)	2.9(4)
O13	0.3564(5)	0.1523(3)	0.0396(3)	3.0(4)
O14	0.7242(9)	0.4572(5)	−0.0422(4)	8.9(8)
C38	0.73201(1)	0.4800(7)	0.0036(6)	6.4(10)

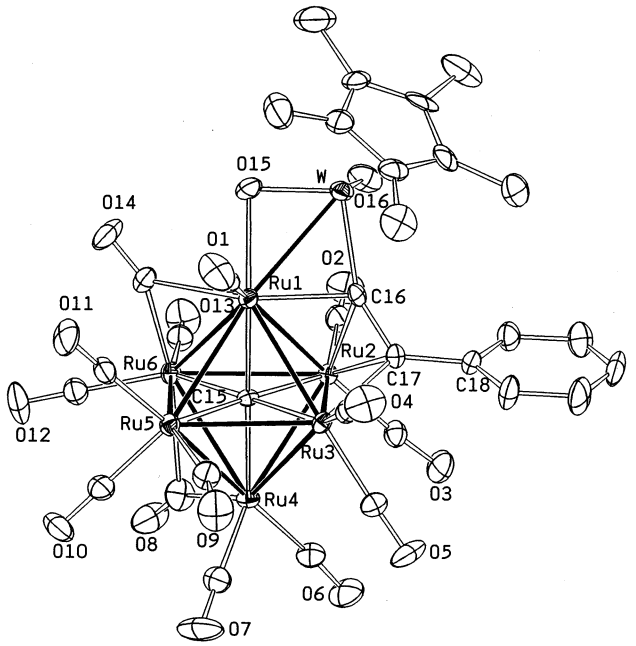

Fig. 1. Molecular structure and atomic labelling scheme of the complex $(C_5Me_5)W(O)_2(CCPh)Ru_6(\mu_6\text{-}C)(CO)_{14}$ (**1**) with thermal ellipsoids shown at the 30% probability level.

lated structural factors are available from the author (Y.C.).

3. Results

The carbido hexaruthenium cluster $Ru_6(\mu_6\text{-}C)(CO)_{17}$ was first treated with 2.5 equiv. of the oxidative decarbonylation reagent Me_3NO in acetonitrile solution. After the removal of acetonitrile solvent and dissolution of the residue in CH_2Cl_2, the addition of acetylide complex $(C_5Me_5)W(O)_2(CCPh)$ produced a brown complex with an empirical formula $(C_5Me_5)W(O)_2(CCPh)Ru_6(\mu_6\text{-}C)(CO)_{14}$ (**1**). This cluster complex was purified by routine TLC separation, and its characterization was fully established by spectroscopic methods including single crystal X-ray diffraction study: FAB mass spectroscopy showed a molecular ion at m/z 1467, which was assigned to a 1:1 combination of the acetylide fragment $(C_5Me_5)W(O)_2(CCPh)$ and the $Ru_6(\mu_6\text{-}C)(CO)_{17}$ unit, with elimination of three CO ligands. In addition, the ^{1}H-NMR spectrum exhibited the signal due to the C_5Me_5 signal at δ 2.02 and three multiplets at δ 746, 7.58 and 7.96 due to the phenyl substituent. The ^{13}C-NMR spectral data are likewise consistent with this formulation, showing a carbide resonance signal at δ 431.4, two acetylide signals at δ 201.6 and 159.6 due to the C_α and C_β atoms in the $\mu_4\text{-}\eta^2$-mode [11], and the corresponding signals derived from the phenyl group and the C_5Me_5 ligand.

A single-crystal X-ray diffraction study has revealed the molecular structure of **1**, and an ORTEP diagram is depicted in Fig. 1. The six ruthenium–metal atoms form an octahedral arrangement which encapsulated the carbido carbon atom C(15). The Ru(1)–C(15) distance (1.997(7) Å) is slightly shorter then the other five Ru–C(15) distances (2.025(7)–2.062(7) Å) due to the presence of a weak σ-donor ligand, O(15) atom, at the *trans* disposition. The W–Ru(1) distance (2.8024(8) Å) is comparable to that observed in several W–Ru mixed metal clusters, suggesting the formation of direct metal–metal bond [12]. The Ru–Ru distances fall in the range 2.7364(9)–3.030(1) Å and the average Ru–Ru distance is 2.881 Å. These bond distances are compatible with the Ru–Ru distances observed in the electron precise, 86 cluster valence electrons, Ru_6 carbido cluster complexes (Scheme 1) [13].

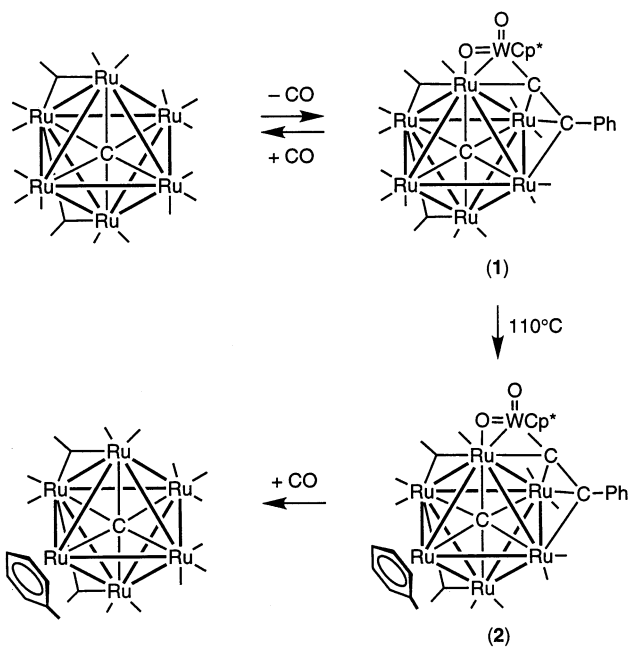

Scheme 1.

In addition, all of the carbonyl ligands except CO(8) and CO(14) are terminal. These two symmetrical bridging CO ligands span the adjacent Ru(4)–Ru(6) and Ru(1)–Ru(6) bonds, respectively, and are joined at the Ru(6) atom trans to each other. The $(C_5Me_5)W(O)_2(CCPh)$ fragment is found to reside on the Ru(1)–Ru(2)–Ru(3) metal triangle with the W atom and one of its oxo ligand, O(15) atom, linked to the Ru(1) atom. The acetylide C(16)–C(17) unit retains its W–C σ-bonding interaction, and is also coordinated to the Ru(2) atom via a π-interaction and to both Ru(1) and Ru(3) atoms via σ-bonding. As the result, the bonding pattern and mode of coordination for the $(C_5Me_5)W(O)_2(CCPh)$ fragment on the Ru_3 metal triangle resemble those observed for the mixed-metal cluster complex $(C_5Me_5)W(O)_2(CCPh)Ru_5(\mu_4\text{-}PPh)(CO)_{12}$ (**3**) reported in our previous study [14]. Furthermore, the $(C_5Me_5)W(O)_2(CCPh)$ unit, which is best considered as

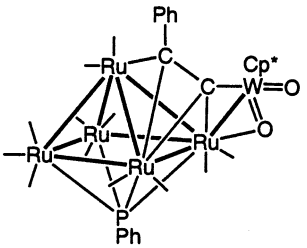

(3)

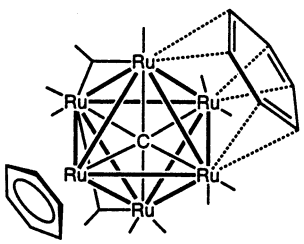

(4)

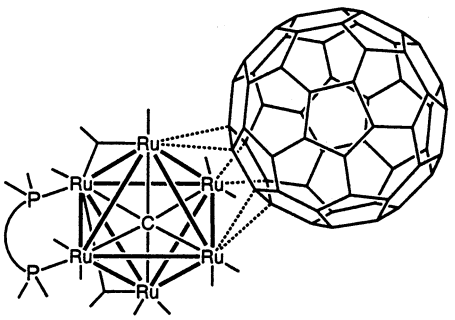

(5)

a six-electron-donor ligand altogether, occupied three adjacent coordination sites which are perpendicular to the Ru(1)–Ru(2)–Ru(3) metal triangle. Thus, the coordination environment for the $(C_5Me_5)W(O)_2(CCPh)$ unit matches that found in the closely related hexaruthenium arene complex $Ru_6(\mu_6\text{-}C)(CO)_{11}(C_6H_6)_2$ (**4**) [15], or even the phosphine substituted C_{60} complex $Ru_6(\mu_6\text{-}C)(CO)_{12}(dppm)(C_{60})$ (**5**) [16]. In these cluster complexes, both the $\mu_3\text{-}\eta^2\text{:}\eta^2\text{:}\eta^2$-arene or the C_{60} fragment, which also serves as the six-electron-donor ligand as a whole, use three conjugated C–C double bonds of the hexagonal ring occupying the identical sites on the $Ru_6(\mu_6\text{-}C)$ octahedral skeleton.

Several studies of **1** were carried out in attempt to expand our understanding of its chemical properties. Treatment of **1** with CO afforded the carbido cluster $Ru_6(\mu_6\text{-}C)(CO)_{17}$ and the free acetylide complex $(C_5Me_5)W(O)_2(CCPh)$ in high yield, suggesting that the acetylide fragment can be reversibly replaced by CO molecules at elevated temperature. Interestingly, when a toluene solution of **1** was heated at 110°C for 8 h under nitrogen we obtained a new cluster complex $(C_5Me_5)W(O)_2(CCPh)Ru_6(\mu_6\text{-}C)(CO)_{11}(C_7H_8)$ (**2**) in 48% yield. The ^{1}H-NMR spectrum of **2** exhibited a methyl signal at δ 2.38 and a complex set of aromatic resonances due to the ligated toluene in the region δ 5.39–5.73, in addition to the signals expected for the $(C_5Me_5)W(O)_2(CCPh)$ fragment. Hence, we speculate that this molecule is produced by incorporation of toluene solvent molecule following elimination of CO ligands. The single-crystal diffraction study was carried out to confirm our postulation and to determine the exact location of the toluene on the hexaruthenium metal framework.

As depicted in Fig. 2, the key structural features of the ligated $(C_5Me_5)W(O)_2(CCPh)$ moiety and the $Ru_6(\mu_6\text{-}C)$ octahedral core of **1** were preserved in complex **2**. In addition, one of the ruthenium atoms, Ru(1), is bonded to the C_6 ring of the expected toluene fragment, which serves as a six-electron-donor to replace the three terminal CO ligands on Ru(5) atom observed in complex **1**. Opposite to this toluene ligand is the Ru(1)–C(12) vector (1.94(1) Å), which is substantially shorter than the rest of the Ru–C(carbide) distances

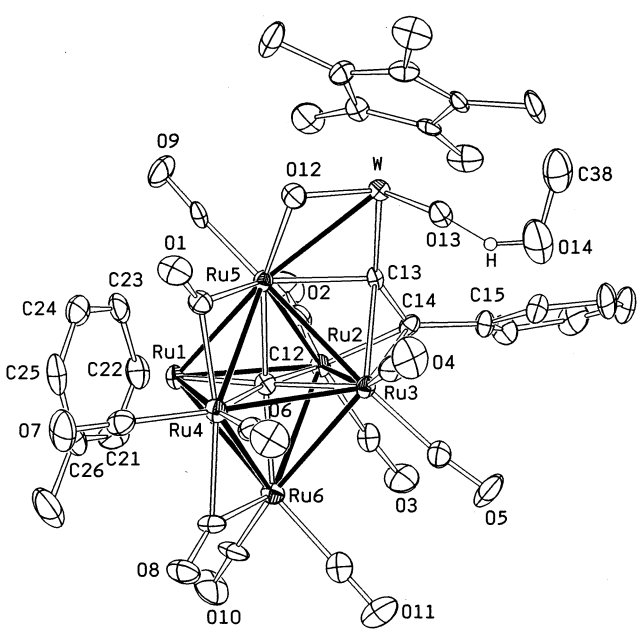

Fig. 2. Molecular structure and atomic labelling scheme of the complex $(C_5Me_5)W(O)_2(CCPh)Ru_6(\mu_6\text{-}C)(CO)_{11}(C_7H_8)\cdot MeOH$ (**2**) with thermal ellipsoids shown at the 30% probability level.

(2.02(1)–2.09(1) Å). Such variation of ruthenium–carbide bond distances suggests that the toluene-to-ruthenium metal bonding is probably the weakest donor interaction with respect to the other ligands on the $Ru_6(\mu_6\text{-C})$ skeleton.

Finally, it is of interest to note that the terminal oxo ligand on the tungsten atom is now bonded to the oxygen atom of the methanol solvate within the asymmetric unit ($O(13)\cdots O(14) = 2.92(1)$ Å), suggesting the presence of extensive hydrogen bonding. However, the $O\cdots O$ bond distance is slightly longer than those observed in the tungsten trioxo complex $[PPN][(C_5Me_5)W(O)_3]\cdot 2H_2O$($O\cdots OH_2 = 2.77$–$2.83$ Å) [17], which is consistent with the fact that complex **2** is a neutral cluster molecule. Therefore, the negative charge density on the terminal oxo ligand will be much lower, and the oxo ligand should be bound less strongly to the hydrogen atom of methanol molecule, and possessing a correspondingly longer $O\cdots O$ distance.

4. Discussion

A summary of the results of this study are shown in the Scheme 1. The reaction of $Ru_6(\mu_6\text{-C})(CO)_{17}$ with $(C_5Me_5)W(O)_2(CCPh)$ gave the formation of cluster complex **1**, which contains a high oxidation state $(C_5Me_5)W(O)_2(CCPh)$ fragment coordinated to a Ru_3 metal triangle of the $Ru_6(\mu_6\text{-C})$ framework. According to its crystal structure, complex **1** is formally produced by the elimination of three CO ligands from $Ru_6(\mu_6\text{-C})(CO)_{17}$, and the attachment of one W=O fragment and the acetylide unit to the $Ru_6(\mu_6\text{-C})$ frame. The vacant coordination sites generated by the addition of Me_3NO to $Ru_6(\mu_6\text{-C})(CO)_{17}$ are not necessarily the same as those occupied by the $(C_5Me_5)W(O)_2(CCPh)$ fragment, because CO migration may occur spontaneously and the final structure is determined by the reaction thermodynamics.

On the other hand, extended heating of **1** in toluene led to the formation of the toluene substituted cluster complex **2**. In this molecule, the $(C_5Me_5)W(O)_2(CCPh)$ and the toluene molecules are linked to the $Ru_6(\mu_6\text{-C})$ framework according to their geometric constraint, e.g. face-capping mode for $(C_5Me_5)W(O)_2(CCPh)$ and terminal η^6-bonding mode for toluene, respectively. It is interesting to point out that only one toluene substituted complex was observed for this reaction, although there is no evidence to suggest that the steric or electronic effects of the $(C_5Me_5)W(O)_2(CCPh)$ fragment will induce such kind of selectivity for toluene coordination on the remote Ru_3 triangular face. We believe that the toluene selects the only ruthenium atom that possesses three terminal CO ligands, and neglects the other ruthenium atoms. Thus, it is the arrangement of CO ligands on the $Ru_6(\mu_6\text{-C})$ framework that caused such unique selectivity for toluene coordination. In addition, the high oxidation-state $(C_5Me_5)W(O)_2$ vertex stayed intact during the conversion from **1** to **2**. It appears to us that the strong W–O multiple bond prohibits the dissociation of oxo ligand and holds up the $(C_5Me_5)W(O)_2$ fragment as an undivided entity throughout the reaction. This is in contrast to the behavior for cluster complexes which contain low valent $(C_5Me_5)W(CO)_n$ vertex, $n = 1$, 2 or 3, where sequential CO dissociation and formation of additional tungsten–metal or tungsten–substrate interactions were typically observed under similar conditions [18].

Finally, the coordination of both acetylide fragment and ligated toluene to ruthenium metal skeleton can be reversed easily. Thus, treatment of **1** with CO in refluxing toluene solution afforded $Ru_6(\mu_6\text{-C})(CO)_{17}$ and $(C_5Me_5)W(O)_2(CCPh)$, while the reaction of **2** with CO gave a mixture of hexaruthenium complexes $Ru_6(\mu_6\text{-C})(CO)_{17}$ and $Ru_6(\mu_6\text{-C})(CO)_{14}(C_7H_8)$, and the starting acetylide complex $(C_5Me_5)W(O)_2(CCPh)$. This result indicates that the thermodynamic stability for the bonding of the $(C_5Me_5)W(O)_2(CCPh)$ and toluene on $Ru_6(\mu_6\text{-C})$ framework is relatively weak. Therefore, in the presence of CO at 110°C, complete replacement by multiple Ru–CO interactions were more favorable. We believe that this reactivity pattern accurately models the bonding situation between a low oxidation-state metal aggregate chemisorbed at the surface of transition metal oxides.

Acknowledgements

We thank the National Science Council of the Republic of China for financial support (Grant No. NSC 87-2113-M007-027-COM).

References

[1] (a) F. Bottomley, L. Sutin, Adv. Organomet. Chem. 28 (1988) 339. (b) J. Xiao, J.J. Vittal, R.J. Puddephatt, L. Manojlovic-Muir, K.W. Muir, J. Am. Chem. Soc. 115 (1993) 7882. (c) W.A. Herrmann, J.D.G. Correia, F.E. Kuehn, G.R.J. Artus, C.C. Romao, Chem. Eur. J. 2 (1996) 168. (d) W.A. Herrmann, F.E. Kuehn, Acc. Chem. Res. 30 (1997) 169.

[2] (a) A. Colombié, J.-J. Bonnet, P. Fompeyrine, G. Lavigne, S. Sunshire, Organometallics 5 (1986) 1154. (b) C.P. Gibson, J.-S. Huang, L.F. Dahl, Organometallics 5 (1986) 1676. (c) A. Ceriotti, L. Resconi, F. Demartin, G. Longoni, M. Manassero, M. Sansoni, J. Organomet. Chem. 249 (1983) C35. (d) H.A. Mirza, J.J. Vittal, R.J. Puddephatt, Inorg. Chem. 34 (1995) 4239. (e) H. Adams, L.J. Gill, M.J. Morris, Organometallics 15 (1996) 464. (f) H. Adams, L. J. Gill, M. Morris, J. Organomet. Chem. 533 (1997) 117. (g) Y. Chi, L.-S. Hwang, G.-H. Lee, S.-M. Peng, J. Chem. Soc. Chem. Commun. (1988) 1456.

[3] R.J. Goudsmit, B.F.G. Johnson, J. Lewis, P.R. Raithby, K.H. Whitmire, J. Chem. Soc. Chem. Commun. (1983) 246.
[4] D. Bright, J. Chem. Soc. Chem. Commun. (1970) 1169.
[5] (a) C.K. Schauer, D.F. Shriver, Angew. Chem. Int. Ed. Engl. 26 (1987) 255. (b) C.K. Schauer, E.J. Voss, M. Sabat, D.F. Shriver, J. Am. Chem. Soc. 111 (1989) 7662.
[6] (a) J.R. Shapley, J.-T. Park, M.R. Churchill, J.W. Ziller, L.R. Beanan, J. Am. Chem. Soc. 106 (1984) 1144. (b) J.T. Park, J.R. Shapley, M.R. Churchill, C. Bueno, Inorg. Chem. 22 (1983) 1579.
[7] G.A. Carriedo, J.C. Jeffery, F.G.A. Stone, J. Chem. Soc. Dalton Trans. (1984) 1597.
[8] (a) Y. Chi, P.-S. Cheng, H.-L. Wu, D.-K. Hwang, S.-M. Peng, G.-H. Lee, J. Chem. Soc. Chem. Commun. (1994) 1839. (b) H.-L. Wu, G.-L. Lu, Y. Chi, L.J. Farrugia, S.-M. Peng, G.-H. Lee, Inorg. Chem. 35 (1996) 6015. (c) Y. Chi, H.-L. Wu, S.-M. Peng, G.-H. Lee, J. Chem. Soc. Dalton Trans. (1997) 1931.
[9] (a) J.T. Park, Y. Chi, J.R. Shapley, M.R. Churchill, J.W. Ziller, Organometallics 13 (1994) 813. (b) Y. Chi, H.-L. Wu, C.-C. Chen, C.-J. Su, S.-M. Peng, G.-H. Lee, Organometallics 16 (1997) 2443.
[10] (a) C.-H. Shiu, C.-J. Su, C.-W. Pin, Y. Chi, S.-M. Peng, G.-H. Lee, J. Organomet. Chem. 151 (1997) 545–546. (b) B.F.G.; Johnson, J. Lewis, M. McPartlin, W.J.H. Nelson, S.W. Sankey, K. Wong, J. Organomet. Chem. 191 (1980) C3.
[11] A.J. Carty, A.A. Cherkas, L.H. Randall, Polyhedron 7 (1988) 1045.
[12] (a) Y. Chi, S.-H. Chuang, B.-F. Chen, S.-M. Peng, G.-H. Lee, J. Chem. Soc. Dalton Trans. (1990) 3033. (b) S.-J. Chiang, Y. Chi, P.-C. Su, S.-M. Peng, G.-H. Lee, J. Am. Chem. Soc. 116 (1994) 11181. (c) C.-J. Su, P.-C. Su, Y. Chi, S.-M. Peng, G.-H. Lee, J. Am. Chem. Soc. 118 (1996) 3289.
[13] (a) R. D. Adams, W. Wu, Polyhedron 11 (1992) 2123. (b) T. Chihara, K. Sawamura, H. Ogawa, Y. Wakatsuki, J. Chem. Soc. Chem. Commun. (1994) 1179. (c) R.L. Mallors, A.J. Blake, S. Parsons, B.F.G. Johnson, P.J. Dyson, D. Braga, F. Grepioni, E. Parisini, J. Organomet. Chem. 532 (1997) 133. (d) A.J. Blake, J.L. Haggitt, B.F.G. Johnson, S. Parsons, J. Chem. Soc. Dalton Trans. (1997) 991.
[14] P. Blenkiron, A.J. Carty, S.-M. Peng, G.-H. Lee, C.-J. Su, C.-W. Shiu, Y. Chi, Organometallics 16 (1997) 519.
[15] (a) P.J. Dyson, B.F.G. Johnson, J. Lewis, M. Martinelli, D. Braga, F. Grepioni, J. Am. Chem. Soc. 115 (1993) 9062. (b) D. Braga, F. Grepioni, S. Righi, P.J. Dyson, B.F.G. Johnson, P.J. Bailey, J. Lewis, Organometallics 11, (1992) 4042.
[16] K. Lee, H.-F. Hsu, J.R. Shapley, Organometallics 16 (1997) 3876.
[17] M.S. Rau, C.M. Kretz, G.L. Geoffroy, Organometallics 12 (1993) 3447.
[18] (a) Y. Chi, C. Chung, Y.-C. Chou, P.-C. Su, S.-J. Chiang, S.-M. Peng, G.-H. Lee, Organometallics 16 (1997) 1702. (b) P.-C. Su, Y. Chi, C.-J. Su, S.-M. Peng, G.-H. Lee, Organometallics 16 (1997) 1870. (c) W.-J. Chao, Y. Chi, C.-J. Way, I. J. Mavunkal, S.-L. Wang, F.-L. Liao, L. J. Farrugia, Organometallics 16 (1997) 3523.